Radiology

ORIGINAL RESEARCH • EVIDENCE-BASED PRACTICE

A Meta-analysis of the Diagnostic Performance of Diffusion MRI for Breast Lesion Characterization

Gabrielle C. Baxter, MPhys • Martin J. Graves, PhD • Fiona J. Gilbert, MD, FRCR, FRCP • Andrew J. Patterson, PhD

From the Department of Radiology, School of Clinical Medicine, University of Cambridge, Box 218, Cambridge Biomedical Campus, Hills Road, Cambridge CB2 0QQ, England (G.C.B., F.J.G.); and Department of Radiology, Addenbrookes Hospital, Cambridge University Hospitals NHS Foundation Trust, Cambridge, England (M.J.G., A.J.P.). Received October 30, 2018; revision requested December 11; revision received March 8, 2019; accepted March 13. **Address correspondence** to F.J.G. (e-mail: *fjg28@medschl.cam.ac.uk*).

Study sponsored by the National Institute for Health Research (Cambridge Biomedical Research Centre at the Cambridge University Hospitals National Health Service Foundation Trust). F.J.G. sponsored by the National Institute for Health Research Senior Investigator award. The views expressed are those of the authors and not necessarily those of the National Health Service, the National Institute for Health Research, or the Department of Health and Social Care.

Conflicts of interest are listed at the end of this article.

Radiology 2019; 00:1–11 • https://doi.org/10.1148/radiol.2019182510 • Content code: MR

Background: Various techniques are available to assess diffusion properties of breast lesions as a marker of malignancy at MRI. The diagnostic performance of these diffusion markers has not been comprehensively assessed.

Purpose: To compare by meta-analysis the diagnostic performance of parameters from diffusion-weighted imaging (DWI), diffusion-tensor imaging (DTI), and intravoxel incoherent motion (IVIM) in the differential diagnosis of malignant and benign breast lesions.

Materials and Methods: PubMed and Embase databases were searched from January to March 2018 for studies in English that assessed the diagnostic performance of DWI, DTI, and IVIM in the breast. Studies were reviewed according to eligibility and exclusion criteria. Publication bias and heterogeneity between studies were assessed. Pooled summary estimates for sensitivity, specificity, and area under the curve were obtained for each parameter by using a bivariate model. A subanalysis investigated the effect of MRI parameters on diagnostic performance by using a Student *t* test or a one-way analysis of variance.

Results: From 73 eligible studies, 6791 lesions (3930 malignant and 2861 benign) were included. Publication bias was evident for studies that evaluated apparent diffusion coefficient (ADC). Significant heterogeneity ($P < .05$) was present for all parameters except the perfusion fraction *(f)*. The pooled sensitivity, specificity, and area under the curve for ADC was 89%, 82%, and 0.92, respectively. The highest performing parameter for DTI was the prime diffusion coefficient (λ_1), and pooled sensitivity, specificity, and area under the curve was 93%, 90%, and 0.94, respectively. The highest performing parameter for IVIM was tissue diffusivity *(D)*, and the pooled sensitivity, specificity, and area under the curve was 88%, 79%, and 0.90. Choice of MRI parameters had no significant effect on diagnostic performance.

Conclusion: Diffusion-weighted imaging, diffusion-tensor imaging, and intravoxel incoherent motion have comparable diagnostic accuracy with high sensitivity and specificity. Intravoxel incoherent motion is comparable to apparent diffusion coefficient. Diffusion-tensor imaging is potentially promising but to date the number of studies is limited.

Online supplemental material is available for this article.

MRI has high sensitivity but lower specificity (93% and 71%, respectively) (1) for the depiction of breast lesions. To improve specificity, the diffusion properties of breast lesions have been investigated. The apparent diffusion coefficient (ADC), measured by using diffusion-weighted imaging (DWI), is increasingly used as a marker in the detection and characterization of breast lesions. The ADC of a malignant lesion is lower than that of a benign lesion because of the restricted diffusion in regions of high cellular density, which is often the result of proliferation of glandular tissue. Multiple studies have set a threshold value for ADC and assessed the diagnostic utility in identifying malignant and benign lesions. Advanced diffusion models attempt to capture more complex aspects of the tumor microenvironment, including diffusion anisotropy and deviation from the monoexponential model due to perfusion effects.

Diffusion-tensor imaging (DTI) is an extension of diffusion MRI that considers the anisotropy and directionality of diffusion because of the effects of restrictions imposed by cell membranes and walls of microstructures. DTI measures orthogonal eigenvectors of diffusion and their eigenvalues, λ_1, λ_2, and λ_3, from which the mean diffusivity, maximal anisotropy index (λ_1–λ_3), and fractional anisotropy can be calculated. DTI has been used in the differential diagnosis of glioblastoma (2), renal cell carcinoma (3), and prostate cancer (4), and in the breast to depict cancer and track the mammary ductal network (5).

Intravoxel incoherent motion (IVIM) was introduced by Le Bihan et al (6) as a method of separating the effects of diffusion and perfusion by fitting a biexponential

Abbreviations

ADC = apparent diffusion coefficient, DTI = diffusion-tensor imaging, DWI = diffusion-weighted imaging, IVIM = intravoxel incoherent motion

Summary

Diffusion-weighted imaging, diffusion-tensor imaging, and intravoxel incoherent motion have comparable diagnostic performance for identification of breast malignancy at MRI.

Key Points

- Diffusion-weighted MRI for depicting malignant breast lesions has good sensitivity and specificity (89% and 82%, respectively), which is similar to that of dynamic contrast agent–enhanced MRI (93% and 71%, respectively).
- Intravoxel incoherent motion MRI has high sensitivity and specificity (88% and 79%, respectively) to identify malignant versus benign breast lesions; diffusion-tensor imaging has slightly better diagnostic accuracy (sensitivity and specificity, 93% and 90%, respectively).
- There is no evidence to suggest that choice of minimum *b* value improves diagnostic performance (ie, 0 or 50 sec/mm^2).

model to the decay of signal by *b* value. In the IVIM model, tissue diffusivity is described by parameter *D*, pseudodiffusion or perfusion is the parameter *D**, and the perfusion fraction is the parameter *f*. This approach has been used in the brain (7), head and neck (8), and prostate (9). It was first used in the breast by Sigmund et al (10) to measure the differences in contribution of the microvasculature between malignant lesions and normal fibroglandular tissue.

Whereas previous meta-analyses have assessed the performance of the ADC model in differentiating between benign and malignant lesions (11–13), more advanced diffusion techniques aim to improve on the results of quantitative DWI. Our meta-analysis compares the diagnostic performance of these advanced diffusion techniques, including DWI, DTI, and IVIM to assess whether they achieve an improvement in diagnostic performance that justifies their higher computational complexity and longer imaging time, which are needed to acquire the range of *b* values or diffusion directions. Because of the lack of standardization in diffusion imaging, a subanalysis investigates how acquisition sequence variations affect diagnostic performance.

Materials and Methods

Literature Search

A search of PubMed and Embase was performed for studies that involved women older than 18 years between January 2000 and March 2018 by one of the authors (G.C.B., with 1 year of experience). The search terms for ADC studies included *breast*, *diffusion*, *apparent diffusion coefficient*, *ADC*, and *monoexponential*. The search terms for DTI studies included *breast*, *diffusion tensor imaging*, and *DTI*. The search terms for IVIM studies included *breast*, *diffusion*, *intravoxel incoherent motion*, *IVIM*, *biexponential*, and *non-mono-exponential*. A search of the lists of references from included studies was also performed.

Study Selection

Studies were included if they met the following eligibility criteria: published in a peer-reviewed journal (abstracts and conference proceedings excluded); in English; data obtained by using a 1.5-T or 3.0-T MRI machine with MRI acquisition information reported; DWI performed and ADC, DTI, or IVIM parameters calculated; the purpose of the study was to investigate the diagnostic performance of ADC, DTI, or IVIM with criteria for classifying benign and malignant lesions clearly stated (ie, threshold value used for a parameter and a computational method used); and sufficient information was reported to extract the number of true-positive, false-negative, false-positive, and true-negative findings classified by using the diagnostic criteria (if the values reported could not be reproduced, the study was excluded); and no limit was defined for age or sample size.

Data Extraction

A data extraction spreadsheet was developed. Data extraction was performed by one author (G.C.B.) and confirmed by a second reviewer (A.J.P., with 12 years of experience). The number of true-positive, false-negative, false-positive, and true-negative findings by using parameters ADC, mean diffusivity, prime diffusion coefficient (λ_1), maximal anisotropy index (λ_1–λ_3), fractional anisotropy, *D*, *f*, and *D** were extracted. For studies that reported multiple sensitivities and specificities, we extracted the method that achieved the highest number of correctly classified lesions (true-positive findings + true-negative findings) to avoid overrepresentation of a sample. For studies that used both a training set and a test set, we extracted the test set values. We extracted reader 1 when studies had multiple readers. For authors with multiple studies published in the same year, we extracted values from only one of the studies.

Other information extracted included the following: mean age and age range or standard deviation (whichever reported), study design, MRI machine and vendor, breast coil used, *b* values (sec/mm^2), repetition time, echo time, matrix size, section thickness, field of view, parallel acceleration (generalized autocalibrating parallel acceleration and sensitivity encoding, and acceleration factor), and fat suppression method. We contacted corresponding authors for missing information.

Data Quality Assessment

The Quality Assessment of Diagnostic Accuracy Studies–2 was performed to assess the quality of studies and likelihood of bias (14). We assessed risk of bias in four domains: patient selection, method of the index test (parameter measurement and use of appropriate threshold to classify lesions), use of histologic analysis as a reference standard, and flow and timing. We constructed funnel plots to visually examine publication bias. An asymmetric or skewed funnel plot suggested the presence of a publication bias. Asymmetry was quantified by using the Egger test (15), and a *P* value of less than .05 indicated publication bias. The degree of heterogeneity between studies was measured by Cochran *Q* test and Higgins I^2 test (16) by using Meta-Disc version 1.4 (Clinical Biostatistics Unit, Hospital Ramon y Cajal, Ma-

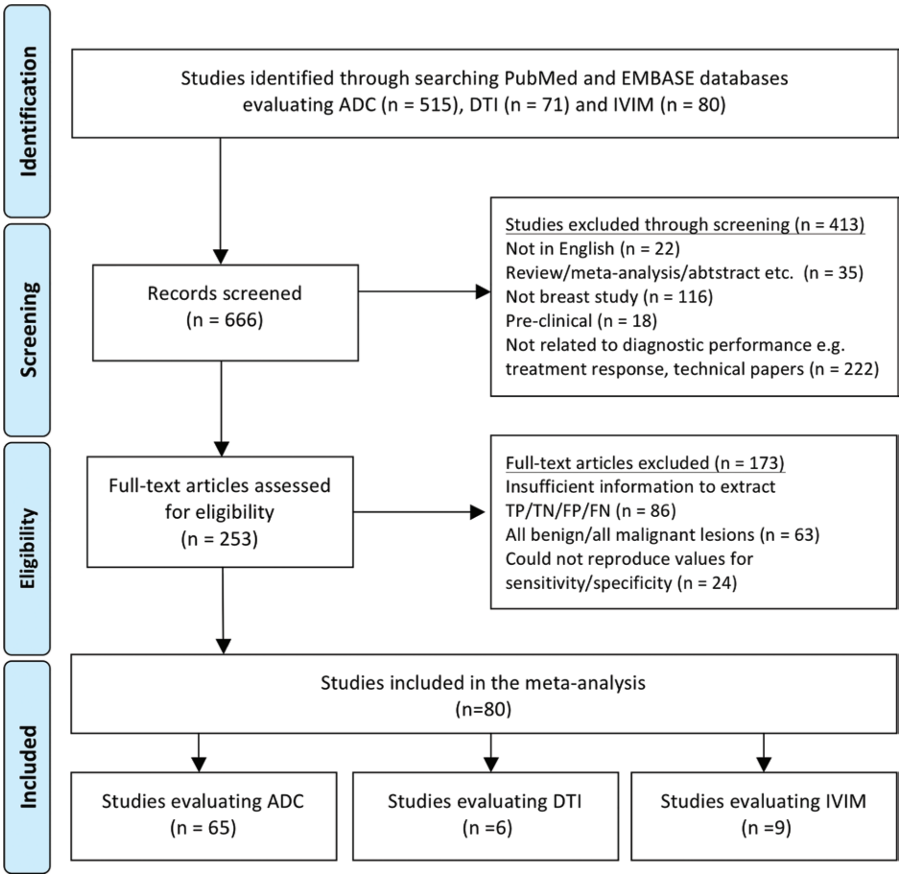

Figure 1: Flowchart for selection and exclusion of studies. ADC = apparent diffusion coefficient, DTI = diffusion-tensor imaging, FN = false negative, FP = false positive, IVIM = intravoxel incoherent motion, TN = true negative, TP = true positive.

Table 1: Combined Approaches by Using DTI and IVIM Parameters

Author	Sensitivity (%)	Specificity (%)	Method
Jiang et al (90)	80.6	74.3	Combined thresholds *D**, *f*
Iima et al (91)	94.7	75.0	Combined thresholds *f*, ADC, *K*
Jiang et al (27)	85.3	90.9	Combined thresholds FA and λ_1–λ_3
Dijkstra et al (22)	92.2	52.2	Combined thresholds *D*, *D**, *f*
Bokacheva et al (53)	85.0	86.0	Linear discriminant analysis *D*, *f*

Note.—λ_1–λ_3 = maximal anisotropy index, ADC = apparent diffusion coefficient, *D* = tissue diffusivity coefficient, *D** = pseudodiffusion coefficient, *f* = perfusion fraction coefficient, FA = fractional anisotropy, *K* = diffusion kurtosis coefficient.

drid, Spain, *http://www.hrc.es/investigacion/metadisc_en.htm*). A *P* value less than .05 for Cochran *Q* test or an I^2 value of greater than 50% indicated statistically significant heterogeneity.

Statistical Analysis

For each of the parameters (ADC; mean diffusivity; λ_1; λ_1–λ_3; fractional anisotropy; and *D*, *f*, and *D**), we constructed forest plots for sensitivity and specificity. We used the bivariate model by Reitsma et al (17) to estimate pooled sensitivities, specificities, and areas under the curve for all parameters and construct summary receiver operating characteristic curves. Analysis was performed by using statistical software (R version 3.1.3; R Foundation for Statistical Computing, Vienna, Austria) by using the mada package.

The effect of *b* value (minimum, maximum, and number used) and other MRI parameters such as field strength, vendor, use of partial field of view, section thickness, and resolution on diagnostic performance (sensitivity, specificity, and area under the receiver operating characteristic curve) was compared by using a Student *t* test, Mann-Whitney *U* test, or a one-way analysis of variance. Method of region-of-interest delineation (use of the whole lesion, a small region of interest, or a single section) was also compared with diagnostic performance by using an analysis of variance. A *P* value less than .05 indicated a statistically significant difference. The data were analyzed in R (R Foundation for Statistical Computing).

Results

Study Selection and Data Extraction

By using the key words, a search of the PubMed and Embase databases returned 515 ADC studies, and 65 of those met the eligibility criteria. A search for DTI returned 71 studies, and six of those met the eligibility criteria. A search for IVIM returned 80 studies, and nine of those met the eligibility criteria. We excluded 413 studies after a review of the titles and abstracts. We reviewed the full text of the remaining 253 studies and excluded 173 that did not meet the eligibility criteria. A total of 80 studies were included in the meta-analysis (5,18–89). Six studies evaluated both ADC and IVIM and one study evaluated both ADC and DTI for all patients included in the study. Figure 1 shows our flowchart of article exclusion. Details of included studies are provided in Table E1 (online). We included 6791 lesions (3930 malignant and 2861 benign) from 73 eligible studies. There was a large range of reported mean ADC values of malignant (0.66–1.50 $\times$ 10^{-3} mm^2/sec) and benign lesions (0.87–2.00 $\times$ 10^{-3} mm^2/sec). Reported diagnostic threshold ADC values ranged from 0.87 $\times$ 10^{-3} mm^2/sec to 2 $\times$ 10^{-3} mm^2/sec. A number of studies with DTI and IVIM used a combined-thresholds approach. The sensitivities and specificities of these studies are in Table 1. Jiang et al (90) reported a sensitivity and specificity for *D** and *f* combined, whereas Bokacheva et al (53) reported a combination of *D* and *f* by using linear discriminant analysis. Dijkstra et al (22) used all three

IVIM parameters and Iima et al (91) reported a combination of *f*, ADC, and diffusion kurtosis coefficient *K*. Jiang et al (27) also reported a combination of fractional anisotropy and the maximal anisotropy index.

Data Quality Assessment

Figure 2 shows the distribution of Quality Assessment of Diagnostic Accuracy Studies–2 scores for risk of bias. The majority of studies had a low risk of bias. Some studies were marked as unclear concerning patient selection because of missing inclusion or exclusion criteria. Common weaknesses included the lack of justification for diagnostic threshold (n = 19), where receiver operating characteristic curves or other analyses were not used, or the lack of consistent use of histologic analysis as the reference standard for all patients (n = 11).

Figure 3 is a funnel plot of ADC studies and it has a funnel-shaped distribution; the lack of studies in the bottom left quadrant indicates publication bias. We measured significant asymmetry by using Egger test (P < .001). Because of the low number of

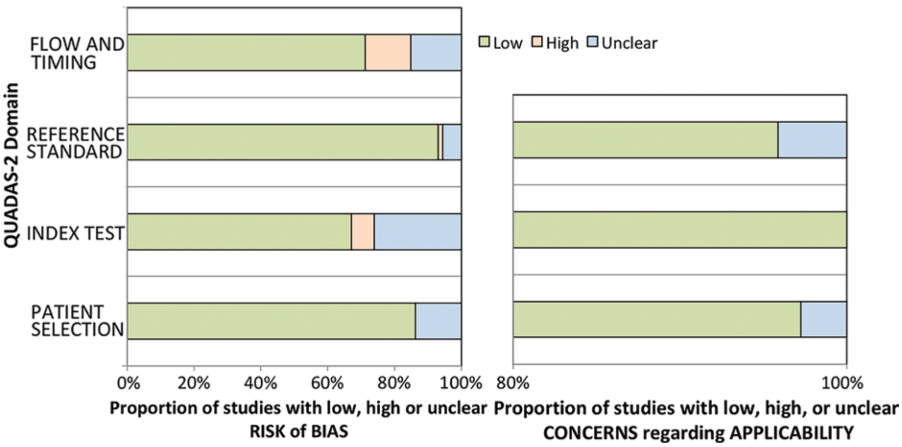

Figure 2: Results of quality assessment for risk of bias and concerns regarding applicability of included studies. Quality assessment of diagnostic accuracy studies (QUADAS-2) scores for each category are expressed by percentages of studies that have a low, high, or unclear risk of bias.

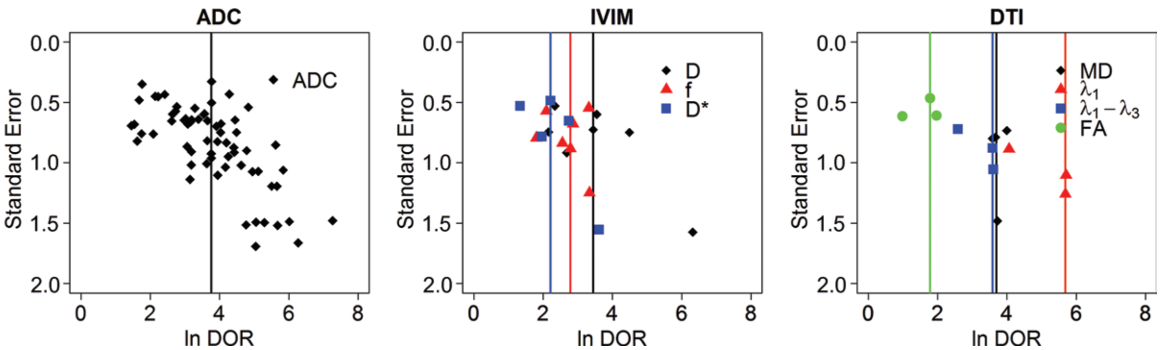

Figure 3: Funnel plots for apparent diffusion coefficient (ADC), intravoxel incoherent motion (IVIM), and diffusion-tensor imaging (DTI) parameters. Log of diagnostic odds ratio (DOR) is plotted against standard error. The vertical line represents the median. IVIM parameters include tissue diffusivity (*D*), perfusion fraction (*f*), and pseudodiffusion (*D**). DTI parameters include mean diffusivity (MD), the prime diffusion coefficient (λ_1), the maximal anisotropy index (λ_1–λ_3), and the fractional anisotropy (FA).

Table 2: Results of Pooled Estimates and Heterogeneity Measures for Diffusion MRI Studies of the Breast

Parameter	No. of Studies	No. of Lesions*	Sensitivity (%)	Heterogeneity: Cochran Q P Value	Heterogeneity: I^2 (%)	Specificity (%)	Heterogeneity: Cochran Q P Value	Heterogeneity: I^2 (%)	AUC
ADC	65	6408 (5892)	89 (87, 91)	<.001	71	82 (78, 85)	<.001	86	0.92 (0.91, 0.93)
D	7	536 (486)	88 (79, 92)	.001	72	79 (64, 89)	<.001	81	0.90 (0.85, 0.96)
f	7	397 (366)	81 (74, 86)	.34	12	76 (64, 85)	.06	50	0.85 (0.81, 0.90)
*D**	5	334 (309)	82 (67, 91)	<.001	87	61 (37, 80)	<.001	85	0.80 (0.74, 0.87)
λ_1	3	201 (181)	93 (80, 98)	.10	56	90 (81, 95)	.59	0	0.94 (0.91, 0.96)
MD	4	262 (247)	90 (79, 96)	.03	66	78 (51, 92)	.001	86	0.92 (0.90, 0.97)
λ_1-λ_3	3	201 (181)	73 (36, 93)	<.001	92	89 (62, 97)	.004	82	0.89 (0.77, 1.00)
FA	3	219 (200)	64 (42, 81)	.003	83	74 (62, 84)	.61	0	0.76 (0.68, 0.87)

Note.—Unless otherwise indicated, data in parentheses are 95% confidence intervals. λ_1 = prime diffusion coefficient, λ_1–λ_3 = maximal anisotropy index, ADC = apparent diffusion coefficient, AUC = area under the receiver operating characteristic curve, *D* = tissue diffusivity, *D** = pseudodiffusion coefficient, *f* = perfusion fraction, FA = fractional anisotropy, I^2 = Higgin I^2 test, MD = mean diffusivity.

* Data in parentheses are number of patients.

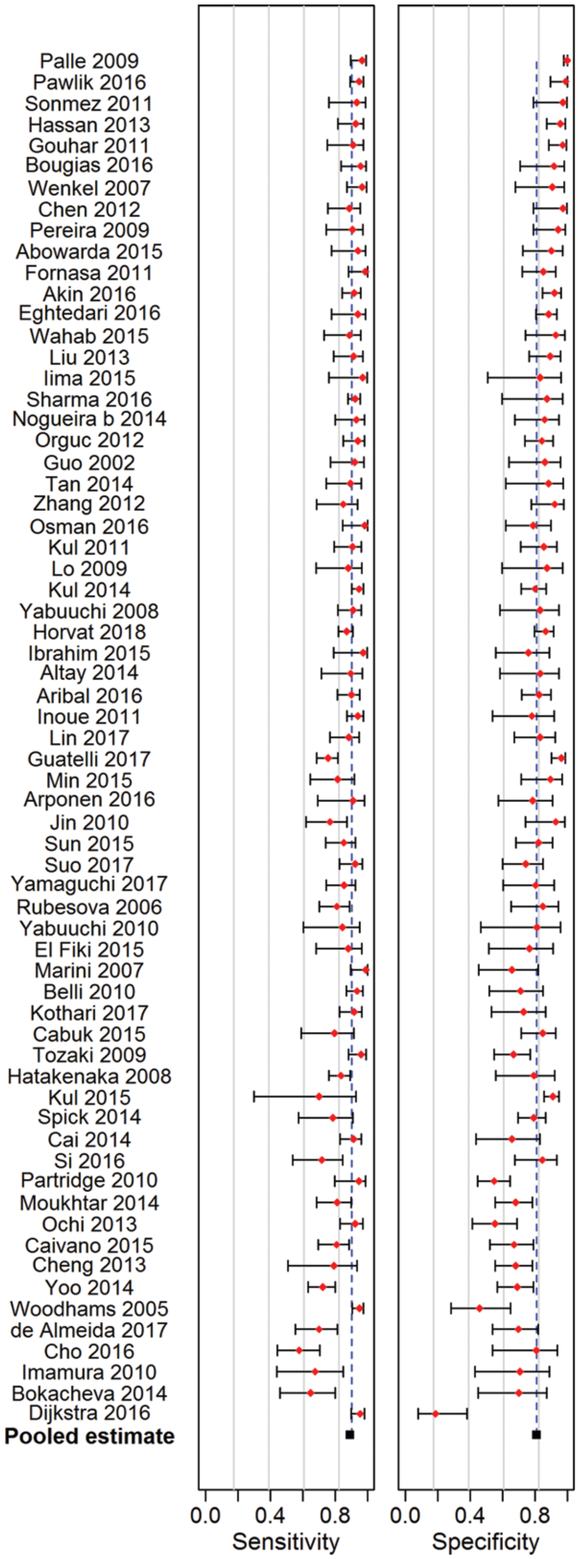

a.

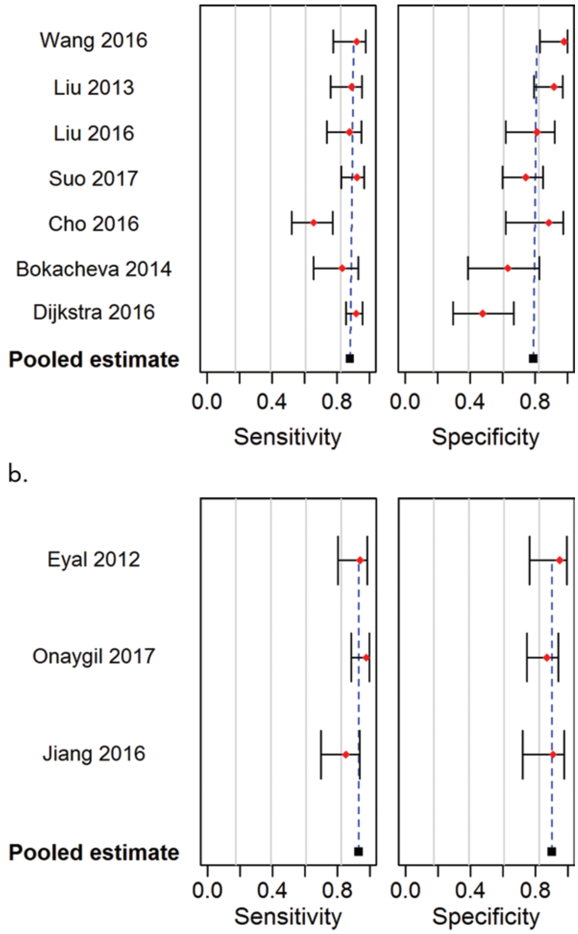

Figure 4: Forest plots of sensitivity and specificity with 95% confidence intervals per study by using **(a)** apparent diffusion coefficient, **(b)** tissue diffusivity, and **(c)** prime diffusion coefficient. Vertical lines denote pooled summary estimates of sensitivity and specificity.

studies for each of the other parameters, funnel asymmetry and Egger test were not assessed.

Statistical Analysis

Table 2 shows the results of the pooled analysis of ADC, DTI, and IVIM parameters. High heterogeneity between studies was measured for most parameters except *f*. I^2 values of 0% were measured for the specificities of λ_1 and fractional anisotropy, however, the low number of studies included in the analysis (three studies for both) resulted in an undefined I^2 value versus significant lack of heterogeneity because Cochran *P* values were .59 and .61, respectively. The pooled area under the curve of the ADC was 0.92. The highest performing parameter for DTI was λ_1, with a pooled area under the curve of 0.94. The highest performing parameter for IVIM was *D*, with a pooled area under the curve of 0.90. Forest plots for sensitivity and specificity for all three parameters are in Figure 4. Summary receiver operating characteristic curves are in Figure 5. Examples of studies that used DTI and IVIM are shown in Figures 6 and 7, respectively.

Table 3 shows the results of the subanalysis. For studies that used ADC, choice of minimum *b* value of 0 sec/mm^2 (n = 56) or 50 sec/mm^2 (n = 9) had no significant effect on sensitivity or specificity (P = .82 and P = .52, respectively). We found no significant differences ($P > .05$) in sensitivity and specificity for maximum *b* value, number of *b* values, field strength, vendor, partial field of view, section thickness, spatial resolution, or method of region of interest delineation.

Discussion

Whereas other meta-analyses assessed the diagnostic performance of the apparent diffusion coefficient (ADC) model (11–13), to our knowledge, ours is the first study to systematically compare all relevant advanced non-Gaussian diffusion techniques with standard diffusion-weighted imaging (DWI) for quantitatively distinguishing benign and malignant lesions. The pooled estimates of sensitivity, specificity, and area under the receiver operating characteristic curve were found to be comparable for ADC, intravoxel incoherent motion (IVIM), and diffusion-tensor imaging (DTI). However, because of the small number of studies included and the large confidence intervals, this meta-analysis lacks the statistical power to conclude that they are diagnostically equivalent.

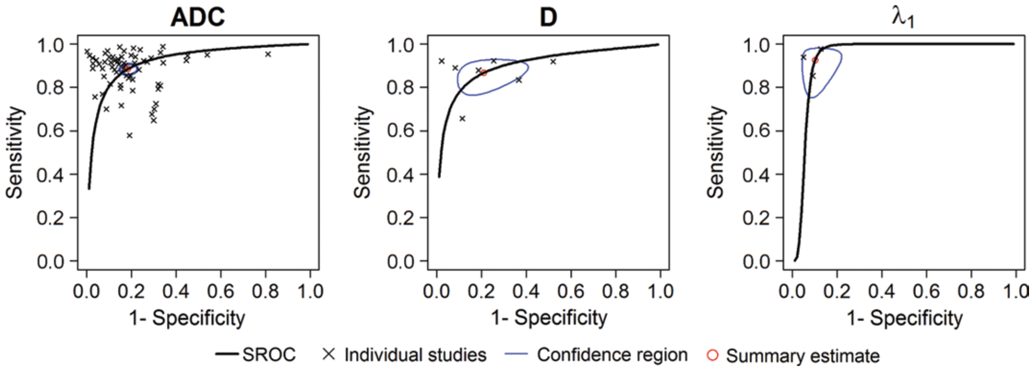

Figure 5: Summary receiver operating characteristics (SROC) curves by using the bivariate model with 95% confidence regions. The pooled area under the curve was 0.92 for the apparent diffusion coefficient (ADC), 0.90 for tissue diffusivity *(D)* and 0.94 for the prime diffusion coefficient (λ_1).

The pooled sensitivities and specificities of DWI, IVIM, and DTI in our meta-analysis were comparable to the pooled sensitivity and specificity of dynamic contrast agent–enhanced MRI (93% and 71%, respectively) (1). Other non-Gaussian diffusion models have been proposed, such as diffusion kurtosis and the stretched exponential model, though these were not investigated because there have been few publications to date. A study by Suo et al (73) showed that kurtosis and stretched exponential achieved a better goodness-of-fit, although the areas under the receiver operating characteristic curve for nonmonoexponential models were comparable to the ADC, which was in accordance with our findings.

DTI lacks standardization in method and reporting of parameters. The prime diffusion direction (λ_1) and the mean diffusivity achieved a diagnostic accuracy equal to or greater than the ADC; however, the number of eligible studies included is low. Whereas it is suggested that reduced structuring in malignant breast lesions should be reflected by a reduced diffusion anisotropy (66), anisotropy measures achieved a mixed diagnostic utility; some studies find no significant difference in fractional anisotropy between malignant and benign lesions (40,57). The number of diffusion directions used ranged from six to 64, though use of the *b* value pair 0 and 1000 sec/mm^2 was the most common (27,40,57,66).

Whereas the increasingly used technique of IVIM in the breast achieves a high diagnostic accuracy, there is also still a lack of consistent methods. There is a large variation in the number and range of *b* values used and in the choice of parameters reported, and studies often use a combined-thresholds approach. Variations in MRI technique prevent determination of generalized threshold values because ADC quantification depends on the choice of *b* values (92). A number of single-center studies have reported their optimal *b* value combination. Bogner et al (93) reported optimal ADC determination and DWI quality at *b* values of 50 and 850 sec/mm^2. Dorrius et al (94) indicated that *b* values of 0 and 1000 sec/mm^2 were optimum, and they found that this *b* value combination achieved the highest percentage difference in ADC of benign and malignant lesions. The *b* values 0 and 1000 sec/mm^2 were the most commonly used in our meta-analysis (n = 29). It has been suggested that the use of more *b* values achieves a better separation of diffusion and perfusion (95), particularly at low *b* values where the contribution of perfusion to signal decay is strongest (6). Whereas this may suggest avoiding low *b* values, the precise *b* value threshold for minimizing perfusion effects has not been standardized and choice of minimum *b* value showed no significant difference in diagnostic performance in studies in our meta-analysis, though this may be because of the lack of statistical power. Also, the diagnostic accuracy of *D*, corresponding to an ADC measurement with effects of perfusion excluded, was comparable to standard DWI. Whereas to our knowledge there is no consensus on whether excluding *b* value of 0 sec/mm^2 or avoiding low *b* values constitutes excluding perfusion effects, both approaches have been shown to have limited effect on diagnostic performance. Choice of fat suppression technique

Table 3: Results of Subanalysis Comparing Studies by Using Apparent Diffusion Coefficient

Parameter	Sensitivity *P* Value	Specificity *P* Value
Minimum *b* value (0 or 50 sec/mm^2)	.82	.52
Maximum *b* value	.08	.71
No. of *b* values	.84	.94
Field strength (1.5 T or 3.0 T)	.14	.64
Vendor	.93	.78
Partial field of view	.79	.43
Section thickness	.60	.72
Spatial resolution	.90	.65
Method of region-of-interest delineation	.66	.57

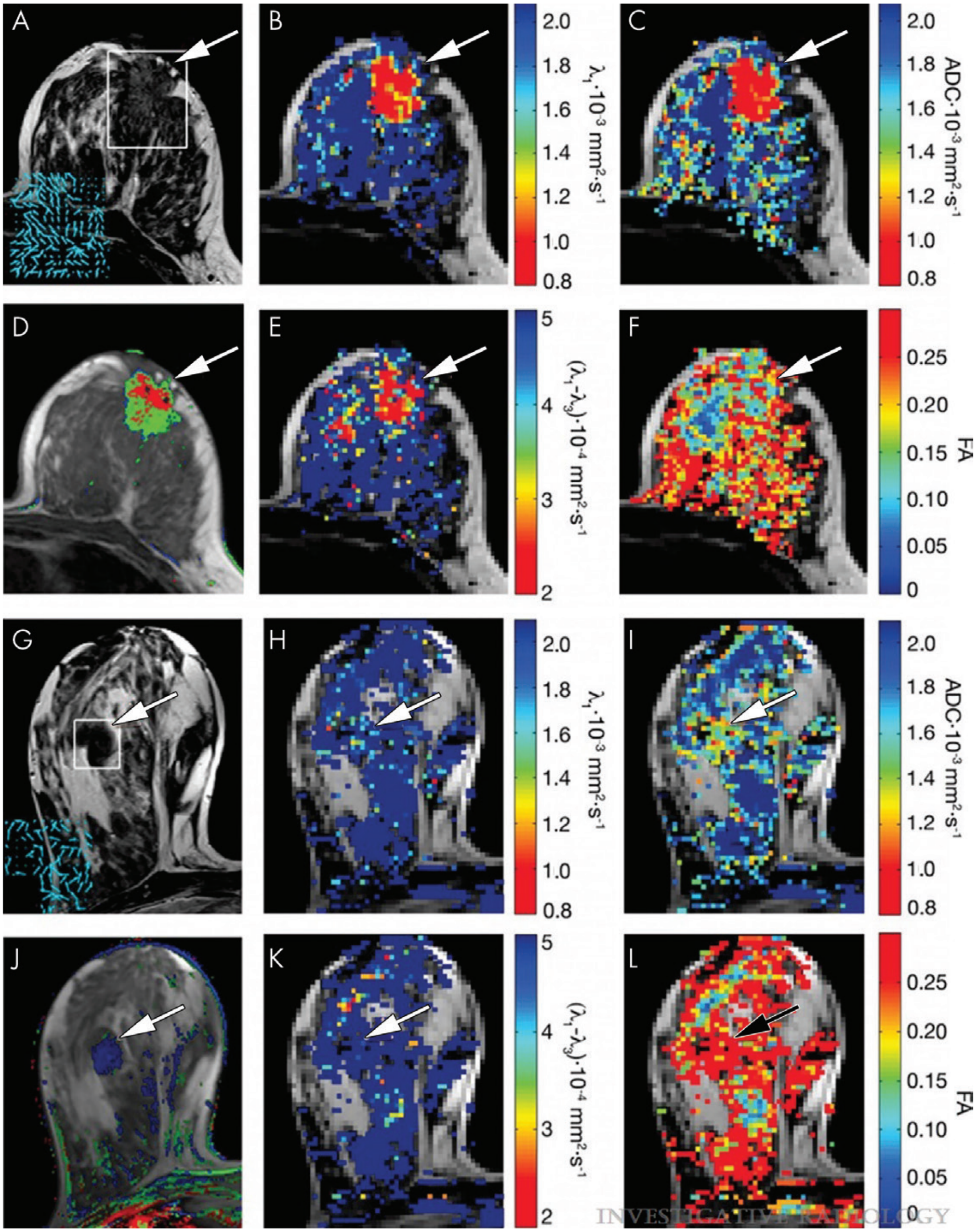

Figure 6: Parametric diffusion maps of breast lesions. Lesions are indicated by arrows. The color-coded maps overlaid on the T2 image were processed with software (Matlab version 7.0.1; Mathworks, Natick, Mass). *A–F*, Invasive ductal carcinoma (37 mm, grade 2) and, *G–L*, fibroadenoma (20 mm). *A*, *G*, T2-weighted images of section at the center of the lesion showing anatomic features. Insert shows a vector map of ν_1 of the region marked by white square on the T2-weighted image. *B, H,* λ_1 maps of the same section as in *A* and *G*, respectively, overlaid on the corresponding T2-weighted image. *C, I,* Apparent diffusion coefficient (ADC) maps of the same section as in *A* and *G*, respectively, overlaid on the corresponding T2-weighted image. *D, J,* Color-coded parametric maps of dynamic contrast-enhanced MRI analysis (three-time-point method) of the same section as in *A* and *G*, respectively, overlaid on a T1-weighted image, show the color-coded contrast-enhanced region. The red pixels in the lesion indicate fast wash-in and fast wash-out, and the green pixels show fast wash-in followed by a plateau; both reflect cancer vascular properties. The blue pixels in the benign lesion indicate a delayed wash-out. *E, K,* λ_1-λ_3 map of the same section as in *A* and *G*, respectively, overlaid on the T2-weighted image. *F, L,* Fractional anisotropy maps of the same section as *A* and *G*, respectively, overlaid on the T2-weighted image. Reprinted, with permission, from reference 5.

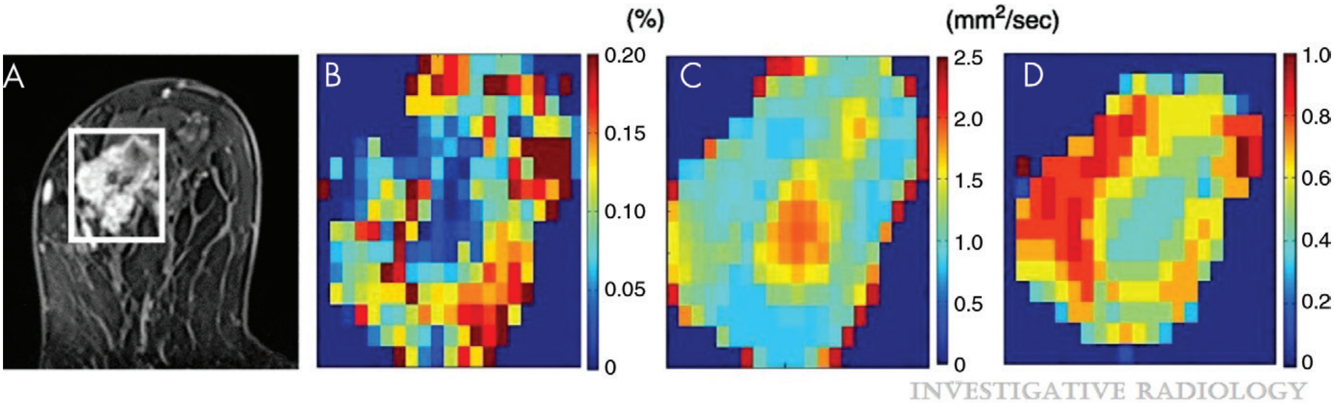

Figure 7: Invasive ductal carcinoma in a 61-year-old woman. *A*, Anatomic contrast-enhanced image. *B*, *f* intravoxel incoherent motion (IVIM) map. *C*, apparent diffusion coefficient (ADC) map. *D*, K map. The white rectangle in *A* shows the area covered by the parametric maps. The high *f* IVIM fraction area at the periphery of the tumor in *B* matches the contrast-enhanced lesion in *A*. The lesion center has low perfusion, which suggests necrosis. An area on the left part of the tumor exhibits a low ADC_0 with high *K* value, which suggests high cellularity (ie, viable malignant component), whereas the central part has a high ADC and low K, suggesting lower cellularity (ie, possible necrosis). Reprinted, with permission, from reference 39.

such as short-τ inversion recovery or spectral adiabatic inversion recovery has been shown to influence image quality and ADC quantification, although diagnostic performance was comparable (96). These discrepancies highlight the importance of choosing similar protocols and methods of data analysis to compare studies across multiple centers.

Our meta-analysis had limitations. First, the low number of studies contributing to the pooled estimates resulted in large confidence intervals, which limited the conclusions that could be drawn from the comparable areas under the curve. Second, overrepresentation of a sample may be a limitation of our pooled estimates because we included multiple studies from the same author that may have used the same patient population. Third, for studies that did not report true-positive, false-negative, false-positive, and true-negative findings, we calculated these outcomes from sensitivity, specificity, and number of malignant and benign lesions. However, many studies were excluded (n = 24) because they resulted in a noninteger number of lesions. Finally, because of the small numbers of publications, we did not include other nonmonoexponential models.

In conclusion, diffusion-weighted imaging, diffusion-tensor imaging (DTI), and intravoxel incoherent motion (IVIM) were able to discriminate between malignant and benign lesions with a high sensitivity and specificity. IVIM was diagnostically comparable to apparent diffusion coefficient (ADC), although the exclusion of perfusion effects that used the tissue diffusion coefficient (*D*) did not improve on the results of the ADC model. DTI achieved a higher accuracy than did ADC, although the number of studies to date is limited. Both IVIM and DTI lack standardization in the reported methods and parameters.

Author contributions: Guarantors of integrity of entire study, G.C.B., F.J.G., A.J.P.; study concepts/study design or data acquisition or data analysis/interpretation, all authors; manuscript drafting or manuscript revision for important intellectual content, all authors; approval of final version of submitted manuscript, all authors; agrees to ensure any questions related to the work are appropriately resolved, all authors; literature research, G.C.B., F.J.G., A.J.P.; statistical analysis, G.C.B., A.J.P.; and manuscript editing, all authors

Disclosures of Conflicts of Interest: **G.C.B.** disclosed no relevant relationships. **M.J.G.** disclosed no relevant relationships. **F.J.G.** Activities related to the present article: disclosed that GE Healthcare provides research support for imaging studies in PET and MRI and the authors are working to improve the diffusion-weighted imaging sequences provided by GE. Activities not related to the present article: disclosed money paid to author from Alphabet to help develop an AI tool for mammography; disclosed money to author's institution from GE Healthcare, Bayer for research support; disclosed money paid to author's institution from GE Healthcare for payment for lectures including service on speaker's bureaus. Other relationships: disclosed no relevant relationships. **A.J.P.** disclosed no relevant relationships.

References

1. Zhang L, Tang M, Min Z, Lu J, Lei X, Zhang X. Accuracy of combined dynamic contrast-enhanced magnetic resonance imaging and diffusion-weighted imaging for breast cancer detection: a meta-analysis. Acta Radiol 2016;57(6):651–660.
2. Wang S, Kim SJ, Poptani H, et al. Diagnostic utility of diffusion tensor imaging in differentiating glioblastomas from brain metastases. AJNR Am J Neuroradiol 2014;35(5):928–934.
3. Feng Q, Fang W, Sun XP, Sun SH, Zhang RM, Ma ZJ. Renal clear cell carcinoma: diffusion tensor imaging diagnostic accuracy and correlations with clinical and histopathological factors. Clin Radiol 2017;72(7):560–564.
4. Gürses B, Tasdelen N, Yencilek F, et al. Diagnostic utility of DTI in prostate cancer. Eur J Radiol 2011;79(2):172–176.
5. Eyal E, Shapiro-Feinberg M, Furman-Haran E, et al. Parametric diffusion tensor imaging of the breast. Invest Radiol 2012;47(5):284–291.
6. Le Bihan D, Breton E, Lallemand D, Aubin ML, Vignaud J, Laval-Jeantet M. Separation of diffusion and perfusion in intravoxel incoherent motion MR imaging. Radiology 1988;168(2):497–505.
7. Yamasaki F, Kurisu K, Satoh K, et al. Apparent diffusion coefficient of human brain tumors at MR imaging. Radiology 2005;235(3):985–991.
8. Yuan J, Yeung DK, Mok GS, et al. Non-Gaussian analysis of diffusion weighted imaging in head and neck at 3T: a pilot study in patients with nasopharyngeal carcinoma. PLoS One 2014;9(1):e87024.
9. Zhang YD, Wang Q, Wu CJ, et al. The histogram analysis of diffusion-weighted intravoxel incoherent motion (IVIM) imaging for differentiating the gleason grade of prostate cancer. Eur Radiol 2015;25(4):994–1004.
10. Sigmund EE, Cho GY, Kim S, et al. Intravoxel incoherent motion imaging of tumor microenvironment in locally advanced breast cancer. Magn Reson Med 2011;65(5):1437–1447.
11. Tsushima Y, Takahashi-Taketomi A, Endo K. Magnetic resonance (MR) differential diagnosis of breast tumors using apparent diffusion coefficient (ADC) on 1.5-T. J Magn Reson Imaging 2009;30(2):249–255.
12. Chen X, Li WL, Zhang YL, Wu Q, Guo YM, Bai ZL. Meta-analysis of quantitative diffusion-weighted MR imaging in the differential diagnosis of breast lesions. BMC Cancer 2010;10(1):693.
13. Shi RY, Yao QY, Wu LM, Xu JR. Breast lesions: diagnosis using diffusion weighted imaging at 1.5T and 3.0T-systematic review and meta-analysis. Clin Breast Cancer 2018;18(3):e305–e320.

14. Whiting P, Rutjes AW, Reitsma JB, Bossuyt PM, Kleijnen J. The development of QUADAS: a tool for the quality assessment of studies of diagnostic accuracy included in systematic reviews. BMC Med Res Methodol 2003;3(1):25.
15. Egger M, Davey Smith G, Schneider M, Minder C. Bias in meta-analysis detected by a simple, graphical test. BMJ 1997;315(7109):629–634.
16. Higgins JPT, Thompson SG, Deeks JJ, Altman DG. Measuring inconsistency in meta-analyses. BMJ 2003;327(7414):557–560.
17. Reitsma JB, Glas AS, Rutjes AWS, Scholten RJPM, Bossuyt PM, Zwinderman AH. Bivariate analysis of sensitivity and specificity produces informative summary measures in diagnostic reviews. J Clin Epidemiol 2005;58(10):982–990.
18. Horvat JV, Durando M, Milans S, et al. Apparent diffusion coefficient mapping using diffusion-weighted MRI: impact of background parenchymal enhancement, amount of fibroglandular tissue and menopausal status on breast cancer diagnosis. Eur Radiol 2018;28(6):2516–2524.
19. Bougias H, Ghiatas A, Priovolos D, Veliou K, Christou A. Whole-lesion apparent diffusion coefficient (ADC) metrics as a marker of breast tumour characterization-comparison between ADC value and ADC entropy. Br J Radiol 2016;89(1068):20160304.
20. Eghtedari M, Ma J, Fox P, Guvenc I, Yang WT, Dogan BE. Effects of magnetic field strength and b value on the sensitivity and specificity of quantitative breast diffusion-weighted MRI. Quant Imaging Med Surg 2016;6(4):374–380.
21. Cho GY, Moy L, Kim SG, et al. Evaluation of breast cancer using intravoxel incoherent motion (IVIM) histogram analysis: comparison with malignant status, histological subtype, and molecular prognostic factors. Eur Radiol 2016;26(8):2547–2558.
22. Dijkstra H, Dorrius MD, Wielema M, Pijnappel RM, Oudkerk M, Sijens PE. Quantitative DWI implemented after DCE-MRI yields increased specificity for BI-RADS 3 and 4 breast lesions. J Magn Reson Imaging 2016;44(6):1642–1649.
23. Liu C, Wang K, Chan Q, et al. Intravoxel incoherent motion MR imaging for breast lesions: comparison and correlation with pharmacokinetic evaluation from dynamic contrast-enhanced MR imaging. Eur Radiol 2016;26(11):3888–3898.
24. Sharma U, Sah RG, Agarwal K, et al. Potential of diffusion-weighted imaging in the characterization of malignant, benign, and healthy breast tissues and molecular subtypes of breast cancer. Front Oncol 2016;6:126.
25. Arponen O, Masarwah A, Sutela A, et al. Incidentally detected enhancing lesions found in breast MRI: analysis of apparent diffusion coefficient and T2 signal intensity significantly improves specificity. Eur Radiol 2016;26(12):4361–4370.
26. Si L, Zhai R, Liu X, Yang K, Wang L, Jiang T. MRI in the differential diagnosis of primary architectural distortion detected by mammography. Diagn Interv Radiol 2016;22(2):141–150.
27. Jiang R, Zeng X, Sun S, Ma Z, Wang X. Assessing detection, discrimination, and risk of breast cancer according to anisotropy parameters of diffusion tensor imaging. Med Sci Monit 2016;22:1318–1328.
28. Pawlik T, Ryś J. Comparison of apparent diffusion coefficient in diffusion-weighted magnetic resonance imaging and morphological assessment of breast tumors. Pol J Pathol 2016;67(4):398–403.
29. Guatelli CS, Bitencourt AGV, Osório CABT, et al. Can diffusion-weighted imaging add information in the evaluation of breast lesions considered suspicious on magnetic resonance imaging? Radiol Bras 2017;50(5):291–298.
30. Akın Y, Uğurlu MÜ, Kaya H, Arıbal E. Diagnostic value of diffusion-weighted imaging and apparent diffusion coefficient values in the differentiation of breast lesions, histpathologic subgroups and correlation with prognostic factors using 3.0 Tesla MR. J Breast Health 2016;12(3):123–132.
31. Aribal E, Asadov R, Ramazan A, Ugurlu MÜ, Kaya H. Multiparametric breast MRI with 3T: effectivity of combination of contrast enhanced MRI, DWI and 1H single voxel spectroscopy in differentiation of breast tumors. Eur J Radiol 2016;85(5):979–986.
32. Osman AM, Shebrya NH. Value of diffusion weighted imaging (DWI) and apparent diffusion coefficient factor (ADC) calculation in differentiation of solid breast lesions. Egypt J Radiol Nucl Med 2016;47(1):363–371.
33. Fusco R, Sansone M, Filice S, et al. Integration of DCE-MRI and DW-MRI quantitative parameters for breast lesion classification. Biomed Res Int 2015;2015:237863.
34. Sun K, Chen X, Chai W, et al. Breast cancer: diffusion kurtosis MR imaging-diagnostic accuracy and correlation with clinical-pathologic factors. Radiology 2015;277(1):46–55.
35. Min Q, Shao K, Zhai L, et al. Differential diagnosis of benign and malignant breast masses using diffusion-weighted magnetic resonance imaging. World J Surg Oncol 2015;13(1):32.
36. Kul S, Oğuz Ş, Eyüboğlu İ, Kömürcüoğlu Ö. Can unenhanced breast MRI be used to decrease negative biopsy rates? Diagn Interv Radiol 2015;21(4):287–292.
37. Caivano R, Villonio A, D' Antuono F, et al. Diffusion weighted imaging and apparent diffusion coefficient in 3 tesla magnetic resonance imaging of breast lesions. Cancer Invest 2015;33(5):159–164.
38. Çabuk G, Nass Duce M, Özgür A, Apaydın FD, Polat A, Orekici G. The diagnostic value of diffusion-weighted imaging and the apparent diffusion coefficient values in the differentiation of benign and malignant breast lesions. J Med Imaging Radiat Oncol 2015;59(2):141–148.
39. Iima M, Yano K, Kataoka M, et al. Quantitative non-Gaussian diffusion and intravoxel incoherent motion magnetic resonance imaging: differentiation of malignant and benign breast lesions. Invest Radiol 2015;50(4):205–211.
40. Yamaguchi K, Nakazono T, Egashira R, et al. Diagnostic performance of diffusion tensor imaging with readout-segmented echo-planar imaging for invasive breast cancer: correlation of ADC and FA with pathological prognostic markers. Magn Reson Med Sci 2017;16(3):245–252.
41. Ibrahim YA, Habib L, Deif A. Role of quantitative diffusion weighted imaging in characterization of breast masses. Egypt J Radiol Nucl Med 2015;46(3):805–810.
42. Abowarda MH, Hasan DI, Elteeh OA. Predictive value of ADC mapping in discriminating probably benign and suspicious breast lesions. Egypt J Radiol Nucl Med 2015;46(2):545–551.
43. Wahab MAKA, Kareem HA, Hassan EE. The utility of diffusion weighted MRI and apparent diffusion coefficient in characterization of breast masses. Egypt J Radiol Nucl Med 2015;46(4):1257–1265.
44. El Fiki IM, Abdel-Rahman HM, Morsy MM. Assessment of breast mass: utility of diffusion-weighted MR and MR spectroscopy imaging. Egypt J Radiol Nucl Med 2015;46(4):1327–1335.
45. Altay C, Balci P, Altay S, et al. Diffusion-weighted MR imaging: role in the differential diagnosis of breast lesions. JBR-BTR 2014;97(4):211–216.
46. Moukhtar FZ, Abu El Maati AA. Apparent diffusion coefficient values as an adjunct to dynamic contrast enhanced MRI for discriminating benign and malignant breast lesions presenting as mass and non-mass like enhancement. Egypt J Radiol Nucl Med 2014;45(2):597–604.
47. Kul S, Eyuboglu I, Cansu A, Alhan E. Diagnostic efficacy of the diffusion weighted imaging in the characterization of different types of breast lesions. J Magn Reson Imaging 2014;40(5):1158–1164.
48. Yoo H, Shin HJ, Baek S, et al. Diagnostic performance of apparent diffusion coefficient and quantitative kinetic parameters for predicting additional malignancy in patients with newly diagnosed breast cancer. Magn Reson Imaging 2014;32(7):867–874.
49. Cai H, Liu L, Peng Y, Wu Y, Li L. Diagnostic assessment by dynamic contrast-enhanced and diffusion-weighted magnetic resonance in differentiation of breast lesions under different imaging protocols. BMC Cancer 2014;14(1):366.
50. Spick C, Pinker-Domenig K, Rudas M, Helbich TH, Baltzer PA. MRI-only lesions: application of diffusion-weighted imaging obviates unnecessary MR-guided breast biopsies. Eur Radiol 2014;24(6):1204–1210.
51. Kothari S, Singh A, Das U, Sarkar DK, Datta C, Hazra A. Role of exponential apparent diffusion coefficient in characterizing breast lesions by 3.0 Tesla diffusion-weighted magnetic resonance imaging. Indian J Radiol Imaging 2017;27(2):229–236.
52. Nogueira L, Brandão S, Matos E, et al. Diffusion-weighted breast imaging at 3 T: preliminary experience. Clin Radiol 2014;69(4):378–384.
53. Bokacheva L, Kaplan JB, Giri DD, et al. Intravoxel incoherent motion diffusion-weighted MRI at 3.0 T differentiates malignant breast lesions from benign lesions and breast parenchyma. J Magn Reson Imaging 2014;40(4):813–823.
54. Tan SLL, Rahmat K, Rozalli FI, et al. Differentiation between benign and malignant breast lesions using quantitative diffusion-weighted sequence on 3 T MRI. Clin Radiol 2014;69(1):63–71.
55. Hassan HHM, Mahmoud Zahran MH, El-Prince Hassan H, Mohamed Abdel-Hamid AE, Abdel Shafy Fadaly G. Diffusion magnetic resonance imaging of breast lesions: Initial experience at Alexandria University. Alexandria J Med 2013;49(3):265–272.
56. Liu C, Liang C, Liu Z, Zhang S, Huang B. Intravoxel incoherent motion (IVIM) in evaluation of breast lesions: comparison with conventional DWI. Eur J Radiol 2013;82(12):e782–e789.
57. Cakir O, Arslan A, Inan N, et al. Comparison of the diagnostic performances of diffusion parameters in diffusion weighted imaging and diffusion tensor imaging of breast lesions. Eur J Radiol 2013;82(12):e801–e806.
58. Cheng L, Bai Y, Zhang J, et al. Optimization of apparent diffusion coefficient measured by diffusion-weighted MRI for diagnosis of breast lesions presenting as mass and non-mass-like enhancement. Tumour Biol 2013;34(3):1537–1545.
59. Ochi M, Kuroiwa T, Sunami S, et al. Diffusion-weighted imaging (b value = 1500 s/mm(2)) is useful to decrease false-positive breast cancer cases due to fibrocystic changes. Breast Cancer 2013;20(2):137–144.

60. Orguc S, Basara I, Coskun T. Diffusion-weighted MR imaging of the breast: comparison of apparent diffusion coefficient values of normal breast tissue with benign and malignant breast lesions. Singapore Med J 2012;53(11):737–743.
61. Chen X, He XJ, Jin R, et al. Conspicuity of breast lesions at different b values on diffusion-weighted imaging. BMC Cancer 2012;12(1):334.
62. de Almeida JRM, Gomes AB, Barros TP, Fahel PE, Rocha MS. Diffusion-weighted imaging of suspicious (BI-RADS 4) breast lesions: stratification based on histopathology. Radiol Bras 2017;50(3):154–161.
63. Zhang B, Zhu B, Li M, et al. Comparative utility of MRI perfusion with MSIDR and DWIBS for the characterization of breast tumors. Acta Radiol 2012;53(6):607–614.
64. Sonmez G, Cuce F, Mutlu H, et al. Value of diffusion-weighted MRI in the differentiation of benign and malign breast lesions. Wien Klin Wochenschr 2011;123(21-22):655–661.
65. Inoue K, Kozawa E, Mizukoshi W, et al. Usefulness of diffusion-weighted imaging of breast tumors: quantitative and visual assessment. Jpn J Radiol 2011;29(6):429–436.
66. Baltzer PAT, Schäfer A, Dietzel M, et al. Diffusion tensor magnetic resonance imaging of the breast: a pilot study. Eur Radiol 2011;21(1):1–10.
67. Kul S, Cansu A, Alhan E, Dinc H, Gunes G, Reis A. Contribution of diffusion-weighted imaging to dynamic contrast-enhanced MRI in the characterization of breast tumors. AJR Am J Roentgenol 2011;196(1):210–217.
68. Fornasa F, Pinali L, Gasparini A, Toniolli E, Montemezzi S. Diffusion-weighted magnetic resonance imaging in focal breast lesions: analysis of 78 cases with pathological correlation. Radiol Med (Torino) 2011;116(2):264–275.
69. Gouhar GK, Zidan E-SH. Diffusion-weighted imaging of breast tumors: Differentiation of benign and malignant tumors. Egypt J Radiol Nucl Med 2011;42(1):93–99.
70. Imamura T, Isomoto I, Sueyoshi E, et al. Diagnostic performance of ADC for non-mass-like breast lesions on MR imaging. Magn Reson Med Sci 2010;9(4):217–225.
71. Jin G, An N, Jacobs MA, Li K. The role of parallel diffusion-weighted imaging and apparent diffusion coefficient (ADC) map values for evaluating breast lesions: preliminary results. Acad Radiol 2010;17(4):456–463.
72. Partridge SC, Demartini WB, Kurland BF, Eby PR, White SW, Lehman CD. Differential diagnosis of mammographically and clinically occult breast lesions on diffusion-weighted MRI. J Magn Reson Imaging 2010;31(3):562–570.
73. Suo S, Cheng F, Cao M, et al. Multiparametric diffusion-weighted imaging in breast lesions: Association with pathologic diagnosis and prognostic factors. J Magn Reson Imaging 2017;46(3):740–750.
74. Belli P, Costantini M, Bufi E, Magistrelli A, La Torre G, Bonomo L. Diffusion-weighted imaging in breast lesion evaluation. Radiol Med (Torino) 2010;115(1):51–69.
75. Yabuuchi H, Matsuo Y, Kamitani T, et al. Non-mass-like enhancement on contrast-enhanced breast MR imaging: lesion characterization using combination of dynamic contrast-enhanced and diffusion-weighted MR images. Eur J Radiol 2010;75(1):e126–e132.
76. Palle L, Reddy B. Role of diffusion MRI in characterizing benign and malignant breast lesions. Indian J Radiol Imaging 2009;19(4):287–290.
77. Pereira FPA, Martins G, Figueiredo E, et al. Assessment of breast lesions with diffusion-weighted MRI: comparing the use of different b values. AJR Am J Roentgenol 2009;193(4):1030–1035.
78. Tozaki M, Fukuma E. ^{1}H MR spectroscopy and diffusion-weighted imaging of the breast: are they useful tools for characterizing breast lesions before biopsy? AJR Am J Roentgenol 2009;193(3):840–849.
79. Lo GG, Ai V, Chan JKF, et al. Diffusion-weighted magnetic resonance imaging of breast lesions: first experiences at 3 T. J Comput Assist Tomogr 2009;33(1):63–69.
80. Yabuuchi H, Matsuo Y, Okafuji T, et al. Enhanced mass on contrast-enhanced breast MR imaging: Lesion characterization using combination of dynamic contrast-enhanced and diffusion-weighted MR images. J Magn Reson Imaging 2008;28(5):1157–1165.
81. Hatakenaka M, Soeda H, Yabuuchi H, et al. Apparent diffusion coefficients of breast tumors: clinical application. Magn Reson Med Sci 2008;7(1):23–29.
82. Marini C, Iacconi C, Giannelli M, Cilotti A, Moretti M, Bartolozzi C. Quantitative diffusion-weighted MR imaging in the differential diagnosis of breast lesion. Eur Radiol 2007;17(10):2646–2655.
83. Wenkel E, Geppert C, Schulz-Wendtland R, et al. Diffusion weighted imaging in breast MRI: comparison of two different pulse sequences. Acad Radiol 2007;14(9):1077–1083.
84. Onaygil C, Kaya H, Ugurlu MU, Aribal E. Diagnostic performance of diffusion tensor imaging parameters in breast cancer and correlation with the prognostic factors. J Magn Reson Imaging 2017;45(3):660–672.
85. Rubesova E, Grell AS, De Maertelaer V, Metens T, Chao SL, Lemort M. Quantitative diffusion imaging in breast cancer: a clinical prospective study. J Magn Reson Imaging 2006;24(2):319–324.
86. Woodhams R, Matsunaga K, Kan S, et al. ADC mapping of benign and malignant breast tumors. Magn Reson Med Sci 2005;4(1):35–42.
87. Guo Y, Cai YQ, Cai ZL, et al. Differentiation of clinically benign and malignant breast lesions using diffusion-weighted imaging. J Magn Reson Imaging 2002;16(2):172–178.
88. Lin N, Chen J, Hua J, Zhao J, Zhao J, Lu J. Intravoxel incoherent motion MR imaging in breast cancer: quantitative analysis for characterizing lesions. Int J Clin Exp Med 2017;10(1):1705–1714.
89. Wang Q, Guo Y, Zhang J, Wang Z, Huang M, Zhang Y. Contribution of IVIM to Conventional Dynamic Contrast-Enhanced and Diffusion-Weighted MRI in Differentiating Benign from Malignant Breast Masses. Breast Care (Basel) 2016;11(4):254–258.
90. Jiang L, Lu X, Hua B, Gao J, Zheng D, Zhou Y. Intravoxel incoherent motion diffusion-weighted imaging versus dynamic contrast-enhanced magnetic resonance imaging: comparison of the diagnostic performance of perfusion-related parameters in breast. J Comput Assist Tomogr 2018;42(1):6–11.
91. Iima M, Kataoka M, Kanao S, et al. Intravoxel incoherent motion and quantitative non-gaussian diffusion MR imaging: evaluation of the diagnostic and prognostic value of several markers of malignant and benign breast lesions. Radiology 2018;287(2):432–441.
92. Peters NHGM, Vincken KL, van den Bosch MAAJ, Luijten PR, Mali WPTM, Bartels LW. Quantitative diffusion weighted imaging for differentiation of benign and malignant breast lesions: the influence of the choice of b-values. J Magn Reson Imaging 2010;31(5):1100–1105.
93. Bogner W, Gruber S, Pinker K, et al. Diffusion-weighted MR for differentiation of breast lesions at 3.0 T: how does selection of diffusion protocols affect diagnosis? Radiology 2009;253(2):341–351.
94. Dorrius MD, Dijkstra H, Oudkerk M, Sijens PE. Effect of b value and pre-admission of contrast on diagnostic accuracy of 1.5-T breast DWI: a systematic review and meta-analysis. Eur Radiol 2014;24(11):2835–2847.
95. Federau C. Intravoxel incoherent motion MRI as a means to measure *in vivo* perfusion: A review of the evidence. NMR Biomed 2017;30(11):e3780.
96. Brandão S, Nogueira L, Matos E, et al. Fat suppression techniques (STIR vs. SPAIR) on diffusion-weighted imaging of breast lesions at 3.0 T: preliminary experience. Radiol Med (Torino) 2015;120(8):705–713.